

UC Davis

UC Davis Previously Published Works

Title

Trapping and Electron Paramagnetic Resonance Characterization of the 5'dAdo• Radical in a Radical S-Adenosyl Methionine Enzyme Reaction with a Non-Native Substrate

Permalink

<https://escholarship.org/uc/item/40q6391r>

Journal

ACS Central Science, 5(11)

ISSN

2374-7943

Authors

Sayler, Richard I

Stich, Troy A

Joshi, Sumedh

et al.

Publication Date

2019-11-27

DOI

10.1021/acscentsci.9b00706

Peer reviewed

Trapping and Electron Paramagnetic Resonance Characterization of the 5′dAdo• Radical in a Radical S-Adenosyl Methionine Enzyme Reaction with a Non-Native Substrate

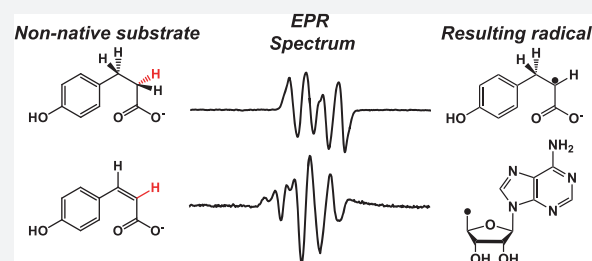
Richard I. Saylor,[†] Troy A. Stich,^{†,‡} Sumedh Joshi,[§] Nicole Cooper,[†] Jared T. Shaw,[†] Tadhg P. Begley,[§] Dean J. Tantillo,[†] and R. David Britt^{*,†}

[†]Department of Chemistry, University of California, Davis, Davis, California 95616, United States

[§]Department of Chemistry, Texas A&M University, College Station, Texas 77842, United States

Supporting Information

ABSTRACT: S-Adenosyl methionine (SAM) is employed as a [4Fe-4S]-bound cofactor in the superfamily of radical SAM (rSAM) enzymes, in which one-electron reduction of the [4Fe-4S]-SAM moiety leads to homolytic cleavage of the S-adenosyl methionine to generate the 5′-deoxyadenosyl radical (5′dAdo•), a potent H-atom abstractor. HydG, a member of this rSAM family, uses the 5′dAdo• radical to lyse its substrate, tyrosine, producing CO and CN that bind to a unique Fe site of a second HydG Fe–S cluster, ultimately producing a mononuclear organometallic Fe–L-cysteine-(CO)₂CN complex as an intermediate in the bioassembly of the catalytic H-cluster of [Fe–Fe] hydrogenase. Here we report the use of non-native tyrosine substrate analogues to further probe the initial radical chemistry of HydG. One such non-native substrate is 4-hydroxy phenyl propanoic acid (HPPA) which lacks the amino group of tyrosine, replacing the C_αH–NH₂ with a CH₂ at the C2 position. Electron paramagnetic resonance (EPR) studies show the generation of a strong and relatively stable radical in the HydG reaction with natural abundance and ¹³C₂-HPPA, with appreciable spin density localized at C2. These results led us to try parallel experiments with the more oxidized non-native substrate coumaric acid, which has a C₂=C₃ alkene substitution relative to HPPA's single bond. Interestingly, the HydG reaction with the *cis-p*-coumaric acid isomer led to the trapping of a new radical EPR signal, and EPR studies using *cis-p*-coumaric acid along with isotopically labeled SAM reveal that we have for the first time trapped and characterized the 5′dAdo• radical in an actual rSAM enzyme reaction, here by using this specific non-native substrate *cis-p*-coumaric acid. Density functional theory energetics calculations show that the *cis-p*-coumaric acid has approximately the same C–H bond dissociation free energy as 5′dAdo•, providing a possible explanation for our ability to trap an appreciable fraction of 5′dAdo• in this specific rSAM reaction. The radical's EPR line shape and its changes with SAM isotopic substitution are nearly identical to those of a 5′dAdo• radical recently generated by cryophotolysis of a pre-reduced [4Fe-4S]-SAM center in another rSAM enzyme, pyruvate formate-lyase activating enzyme, further supporting our assignment that we have indeed trapped and characterized the 5′dAdo• radical in a radical SAM enzymatic reaction by appropriate tuning of the relative radical free energies via the judicious selection of a non-native substrate.



INTRODUCTION

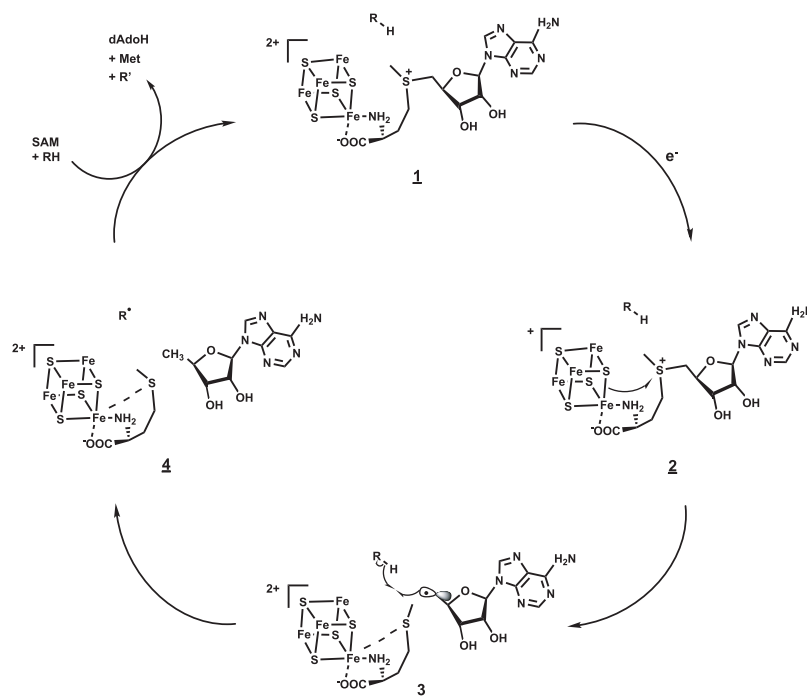
Adenosylcobalamin (AdoCbl) in vitamin B12 enzymes and [4Fe-4S]-bound S-adenosyl methionine (SAM) in the radical SAM (rSAM) superfamily of enzymes^{1–3} are both capable of generating the 5′-deoxyadenosyl radical (5′dAdo•), which is a potent H-atom abstractor that can initiate a wide array of difficult chemical transformations. In the AdoCbl enzymes, the Ado group is bound via its C5′ as an axial ligand to the corrin-bound cobalt, and homolytic Co–C bond cleavage generates the 5′dAdo• radical. In the rSAM enzymes, SAM is bound at an open coordination position of an Fe of a site-differentiated [4Fe-4S] cluster, where cysteines provide ligands to the other three irons, typically presented in a canonical Cys-X₃-Cys-X₂-Cys sequence (Scheme 1, 1). Here the 5′dAdo• radical is generated by one-electron reduction of the [4Fe-4S] cluster,

which leads to a homolytic cleavage between the S atom of methionine and the C5′ of adenosine (Scheme 1, 2). The resulting 5′dAdo• immediately abstracts an H-atom from a substrate molecule (Scheme 1, 3) to generate the primary substrate radical and dAdoH (Scheme 1, 4). A given rSAM enzyme binds the substrate in the active site precisely in order to achieve regio- and stereofidelity in this H-atom abstraction by 5′dAdo•. The rSAM radical chemistry has been harnessed by an enormous variety of enzymes (<http://sfl.d.rvbi.ucsf.edu/django/superfamily/29/>) carrying out a range of challenging biochemical reactions. Electron paramagnetic resonance (EPR) spectroscopy has been used to characterize a variety

Received: July 15, 2019

Published: September 25, 2019

Scheme 1. A Radical SAM Enzyme Mechanism Begins with the Formation of the 5'dAdo• Radical by 1e⁻ Reductive Cleavage of a [4Fe-4S] Cluster-Bound SAM, Which Then Abstracts an H-Atom from Substrate (R)^a



^aThe cysteine ligands to the other three irons of the [4Fe-4S] cluster are omitted for simplicity.

of substrate radicals formed in such rSAM enzyme reactions, but to date there is no verified report of the detection of the primary, but evanescent, 5'dAdo• radical (vide infra).

Recently, there was an important breakthrough in generating the 5'dAdo• radical via cryogenic photolysis of a rSAM center as an alternative to trapping it in an enzymatic reaction.⁴ Here Broderick, Hoffman, and co-workers illuminated the rSAM enzyme pyruvate formate-lyase frozen with a prereduced [4Fe-4S]-SAM cluster for ~1 h with 450 nm illumination at a temperature of 12 K. Using isotopically labeled SAM and employing EPR and electron nuclear double resonance (ENDOR) spectroscopies, these investigators clearly demonstrated that they produced and stabilized the 5'dAdo• radical with this cryophotolysis procedure. Their experimental results in turn serve as the basis for density functional theory (DFT) calculations to obtain an optimized structure for the cryophotolysis generated form of the 5'dAdo• radical.

Here we report the direct trapping of the 5'dAdo• radical in an actual radical SAM enzyme reaction along with its EPR characterization using isotopically labeled S-adenosyl methionine. The enzyme, HydG, is a rSAM tyrosine lyase used to generate the CO and CN ligands ultimately incorporated in the catalytic H-cluster of [Fe-Fe] hydrogenase.⁵⁻⁸ We have previously used EPR spectroscopy of the HydG reaction with isotopically labeled tyrosine, frozen rapidly to trap reaction intermediates, as a probe of the radical SAM chemistry driving the lysis of tyrosine.⁹ The use of specific magnetic nuclear substrate labels is crucial to definitively assign any detected radical in such experiments. In this case, the EPR spectrum of the trapped radical was assigned to a 4-hydroxidobenzyl radical produced following C_α-C_β bond lysis of some initial tyrosine radical produced by the 5'dAdo•-driven H-atom abstraction. There has been some debate concerning the specific identity of

this initial tyrosine radical tied to which specific tyrosine H-atom is abstracted in its generation⁹⁻¹³ (vide infra).

We are now exploring the use of tyrosine analogues as non-native substrates in order to further understand the radical chemistry associated with tyrosine lysis by the 5'dAdo• radical generated in HydG. The likelihood that an amino group hydrogen is the target of the HydG H-atom transfer was suggested by a recent X-ray structure of NosL, a rSAM tryptophan lyase¹⁴ which carries out an analogous C_α-C_β bond cleavage for its tryptophan substrate. To date, all HydG structures lack bound substrate tyrosine, but based on the NosL structure an analogous substrate tyrosine binding site can be modeled (Figure 1).¹⁵

This picture led us to select 4-hydroxy phenyl propanoic acid (HPPA), with a simple CH₂ replacing the C_αH-NH₂ of tyrosine (Figure 2), as a non-native substrate of interest. We show here that HydG generates an HPPA-derived radical with majority spin density at the C2 carbon that substitutes for the tyrosine C_αH-NH₂ moiety. On the basis of these specific EPR results, we can conclude that HPPA binds in a closely analogous site to that of the native substrate tyrosine, preserving HydG's specific rSAM regioselectivity. This led us to try a further non-native substrate experiment, using coumaric acid which has a C₂=C₃ alkene substitution relative to HPPA's single bond (Figure 2). We reasoned, supported by DFT calculations, that this alkane-to-alkene substitution would elevate the energy barrier for an analogous C2 H-atom abstraction, leading to a possible trapping of the initial 5'dAdo• radical. This indeed is the case for the use of the *cis-p*-coumaric acid isomer as a non-native substrate: we trap a new radical species, and EPR spectra obtained with specific SAM isotope labels shows this to be the 5'dAdo• radical, with spin density highly localized at C5'. This is the first isotope-confirmed example of a 5'dAdo• radical trapped in a radical SAM

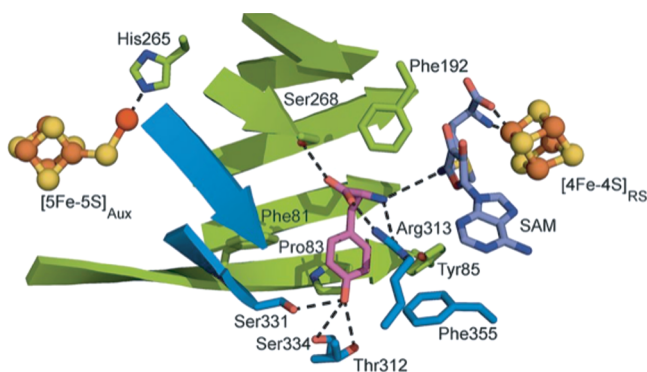


Figure 1. Fe–S centers in the HydG X-ray crystal structure¹⁵ including a model of the tyrosine docking site (PDB: 4WCX) based on the tryptophan binding site of NosL.¹⁴ The [4Fe-4S] center with bound SAM is on the right side of the figure. The cluster on the left is a unique cluster with a fifth “dangler” Fe coupled to a [4Fe-4S] cluster, later shown to be via ligation by an exogenous cysteine.⁴⁴ This figure is reproduced from Dinis et al.¹⁵ with permission from PNAS. Copyright 2015 National Academy of Sciences.

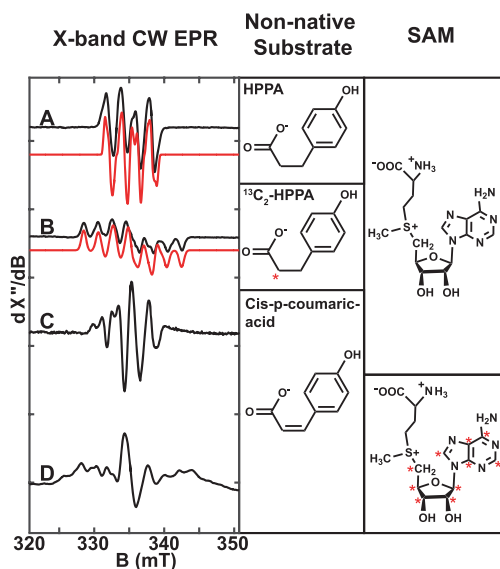


Figure 2. X-band CW EPR spectra of organic radicals generated by HydG. (A) shows the spectrum resulting from a reaction mixture of HydG 100 μ M, DTH 1 mM, 4-hydroxy phenyl propanoic Acid (HPPA) 300 μ M, S-adenosyl methionine (SAM) 300 μ M, in HEPES buffer (pH 7.5). (B) is identical but for a single ¹³C at the C2 position (¹³C 2-HPPA). (C) and (D) are the subtraction spectra of the reaction mixture of HydG 100 μ M, DTH 1 mM, *cis-p-coumaric acid* 300 μ M, and (C) natural abundance (N.A.) SAM or (D) S-adenosyl-(2,4,5,6,8,1',2',3',4',5'-¹³C₁₀)-methionine, 300 μ M, in HEPES buffer (pH 7.5). Spectra C and D are generated by subtracting the spectra acquired at 60 K (accounting for a 1/T dependence of the signal intensity) from the spectra acquired at 40 K to remove an unassigned signal. Spectrometer configuration: frequency 9.4 GHz, (A) and (B) power 200 μ W, (C) and (D) power 2 mW. The red traces (A) and (B) are simulations using the same *g*-tensor = [2.002 2.004 2.005] and with the same set of three protons hyperfine tensors and corresponding Euler angles A (Ha) = [−24 −57 −90.8], Euler angle (Hb) = [3 10 −80]°, A(Hb) = [108 105.8 121.5], Euler angle (Hc) = [40 55 −40]°, A(Hc) = [6 0 6], Euler angle (Hc) = [0 0 0]°, but with the addition of a single ¹³C hyperfine tensor, A(¹³C) = [11 210 11], Euler angle (¹³C) = [5 34 95]° in trace B.

reaction, in this case by using this rationally selected non-native substrate, *cis-p-coumaric acid*.

RESULTS AND DISCUSSION

Our initial foray into using non-native substrates was motivated in part by the difference of opinion in the literature concerning the identity of the primary tyrosine radical of the HydG rSAM reaction, which is tied to the identity of the specific tyrosine H-atom abstracted by the 5' dAdo[•] radical. A number of papers discussing the radical mechanism of HydG and/or the related tyrosine lyase ThiH have modeled the initial tyrosine radical as a neutral tyrosine radical formed by H-atom abstraction of the OH hydrogen of the phenol group.^{9–13} Mass spectrometry of the dAdoH species formed as a result of 5' dAdo[•]-driven H-atom abstraction from tyrosine shows that the shows that the H-atom originates from a solvent exchangeable position,^{9,13} consistent with its assignment to the OH. However, it is worth noting that such neutral tyrosine radicals are quite stable, either as redox active residues in proteins or isolated species in solution,^{16–21} and they do not fragment like the substrate tyrosine of HydG. Moreover they are generally not generated via H-atom abstraction, but rather via a proton coupled electron transfer mechanism. For example, the highest potential neutral tyrosine radical in biology is the Y_Z[•] radical of photosystem II that serves as an electron transfer intermediate between the photooxidized chlorophyll species P₆₈₀⁺ and the 4Mn–Ca cluster that oxidizes water: here there is no H-atom abstraction, but a transfer of a proton to and from a nearby histidine residue during the oxidation and reduction electron transfers.^{16,22}

The other candidate for an exchangeable H-atom on tyrosine is the amino group. As noted in the introduction, the likelihood that an amino hydrogen is the target of the HydG H-atom transfer was suggested by a recent X-ray structure of rSAM tryptophan lyase NosL.¹⁴ The NosL structure includes a bound tryptophan (which of course lacks the OH group of tyrosine) oriented to favor rSAM based H-atom abstraction from the amino group. The authors conclude that NosL initiates its C_α–C_β bond cleavage via a resulting aminyl radical and suggest a similar mechanism for the tyrosine lyases ThiH and HydG. Hydrogen atom abstraction from the tryptophan amino group was confirmed with biochemical experiments.²³ Although the current HydG structure lacks bound substrate tyrosine, bound tyrosine can be modeled based on the tryptophan bound crystal structure of homologue NosL (Figure 1).¹⁵ Comparing the NosL substrate crystal structure with the HydG crystal structure, we see that the amino acids Pro 88, Tyr 90, Arg 323, and Ser 340 in NosL, which are necessary in substrate-binding, correspond to Pro 83, Tyr 85, Arg 313, and Ser 331/334 in HydG and are conserved, where Pro 83 will make a CH– π interaction with the phenyl ring of the substrate tyrosine, Tyr 85 is a H-bond partner with the amino group, Arg 313 acts as a H-bond partner with the carboxyl group, and Ser 331/334 acts as a H-bond partners with the OH of the phenyl group.

Our use of non-native substrates to probe the radical chemistry of HydG initially focused on 4-hydroxy phenyl propanoic acid (HPPA), where the C_αH–NH₂ of tyrosine is replaced by CH₂ (Figure 2). The X-band continuous wave (CW) EPR spectra of HydG frozen reaction intermediates are shown in Figure 2. Trace A shows the spectrum of the radical trapped with natural abundance HPPA (~60 s freeze quench time). We see four well-defined hyperfine peaks that can be

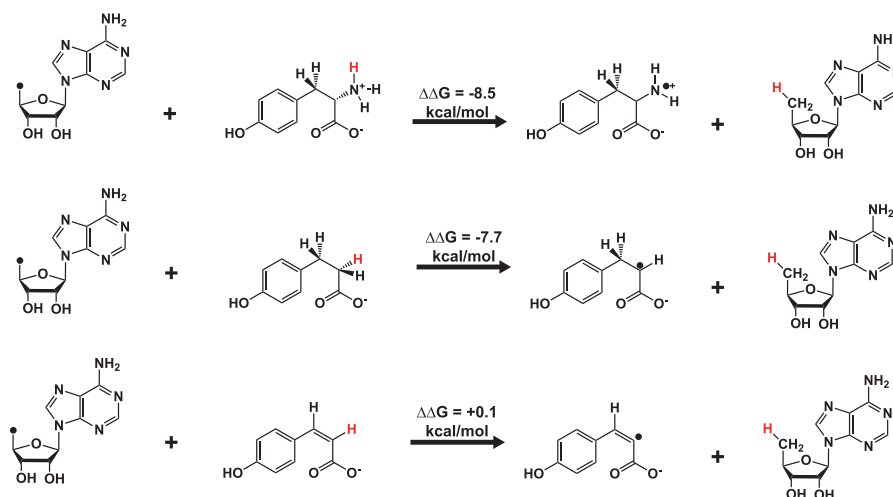


Figure 3. Qualitative depiction of the reaction free energies calculated by DFT (see SI Section V) for H-atom abstraction by free S' dAdo \cdot from the amino group of the zwitterionic state of tyrosine (top), from C2 of 4-hydroxyphenyl propanoic acid (HPPA) (middle), and from C2 of *cis-p*-coumaric acid (bottom). ΔG values are in kcal/mol units.

simulated with two inequivalent ^1H hyperfine couplings (red trace). To prove that this strong radical signal arises from HPPA and to test our specific hypothesis that the radical will be generated by an H-atom abstraction at the C2 site in analogy to amino H abstraction in the native substrate tyrosine, we synthesized HPPA with a single ^{13}C (spin $I = 1/2$) at the C2 position. Trace B shows the EPR spectrum of this ^{13}C HPPA, well simulated (red trace) with a strong hyperfine interaction to the $^{13}\text{C}2$ that further splits the four hyperfine peaks of the unlabeled HPPA radical. Mass spectrometry of dAdoH with these HPPA reactions run in buffer with natural abundance water versus $^2\text{H}_2\text{O}$ shows that the abstracted H-atom is not exchangeable with HPPA as a substrate, eliminating the phenol OH group as the abstracted hydrogen and consistent with radical labeling experiment indicating a C2–H hydrogen abstraction (Figure S5). (Details of the radical chemistry revealed by C2 deuteration will be discussed in an upcoming article.) Additionally, no products other than HPPA itself were detected by mass spectrometry. Furthermore, the HPPA-derived radical appears quite stable compared to the time scale of tyrosine cleavage and formation of the 4-hydroxidobenzyl radical.⁹ These findings imply that the HPPA primary substrate radical does not fragment and is instead quenched by relatively slow H-atom reabstraction from the protein or dAdoH. This HPPA-derived radical intensity is several fold higher than that of the 4-hydroxidobenzyl radical obtained with HydG with the native substrate tyrosine.

For the natural abundance HPPA-derived radical (Figure 2A), the quartet-pattern EPR signal is well simulated with a g -matrix of [2.002 2.004 2.005] and with two inequivalent protons with hyperfine values (MHz) of $|A(\text{H}_a)| = [30\ 57\ 90]$ and $|A(\text{H}_b)| = [107\ 118\ 130]$. The isotropic component of the hyperfine coupling, a_{iso} for H_b is 110 MHz, nearly twice that for H_a ($a_{\text{iso}} = 59$ MHz), which results in the apparent 1:1:1:1 intensity quartet EPR spectrum. The rhombicity of the H_a hyperfine tensor suggests this proton belongs to an atom bound directly to the spin carrying center,²⁴ likely localized to a single aliphatic carbon, consistent with a radical resulting from H-atom abstraction from C2 or C3 of HPPA, but not from the phenol OH group. The EPR signature of the radical generated from the ^{13}C 2-HPPA substrate, with the quartet features each further split into doublets due to the addition of a

strongly coupled ^{13}C (with $A(^{13}\text{C}) = [-20\ 215\ -20]$), in turn localizes the spin density to the C2 carbon (Figure 2B).

This experimentally determined ^{13}C hyperfine tensor can be used to determine the distribution of the unpaired electron density using empirical methods developed using well-known model systems. The hyperfine tensor A is composed of isotropic (a_{iso}) and anisotropic (T) components, where $A = a_{\text{iso}} + T$. The isotropic component is due to the Fermi contact interaction and is proportional to the unpaired electron density at the nucleus. The anisotropic component T occurs via through-space interactions of distant spin centers with the nuclear spin (T_{nonloc}) and dipolar interactions from partially occupied p and d orbitals centered on the atom (T_{loc}). The anisotropic component of the hyperfine tensor of $^{13}\text{C}2$ ($T(\text{C}2)$) can be used to calculate the spin density in the 2p orbital of C2 ($\rho_{\text{C}2}$). $T(\text{C}2)$ is dominated by the dipolar interaction of the singly occupied 2p orbital with the ^{13}C at C2, and thus $T_{\text{nonloc}}(\text{C}2)$ is a minor component and $T = T_{\text{loc}}$ is a good approximation. The measured $^{13}\text{C}2$ hyperfine parameters produce values of $a_{\text{iso}} = 58$ MHz and $T = [-78\ -78\ 157]$ which can be used to calculate the unpaired electron density in the 2p orbital of C2 by the method of Morton and Preston,²⁵ which relates the spin density to the elements of the T_{loc} hyperfine tensor, here approximately equal to the measured elements of T , with the established value of $P = 268.5$ MHz:

$$T(\text{C}) = \rho_{\text{C}} \begin{pmatrix} -\frac{2}{5}P \\ \frac{2}{5}P \\ +\frac{4}{5}P \end{pmatrix}$$

This analysis of our experimental ^{13}C hyperfine affords an assignment of $\rho_{\text{C}2} = 0.73$. The $^1\text{H}_a$ hyperfine simulation parameters (caption of Figure 2) can also be used to calculate $\rho_{\text{C}2}$. The $^1\text{H}_a$ hyperfine coupling is assigned to the proton of a hydrogen bound to C2 of HPPA with hyperfine matrix of $|[30\ 57\ 90]|$ (MHz) giving an $|a_{\text{iso}}|$ of 59 MHz. We can use the McConnell relationship²⁶ between the carbon 2p $_z$ spin density and the observed ^1H a_{iso} value:

$$a_{\text{iso}} = Q\rho_{\text{C}}$$

where Q has the numerical value of 1631 MHz. The measured hyperfine coupling corresponds to $\rho_{\text{C}2} = 0.94$. Thus, both the ^{13}C and ^1H hyperfine analyses point to a large spin density localized on the C2 carbon, with a mean spin density of $\bar{\rho}_{\text{C}2} = 0.8(0.15)$: thus, the majority of the spin density on the HPPA-derived radical is at the C2 carbon which was specifically ^{13}C -labeled due to its spatial correspondence to the $\text{C}_\alpha\text{NH}_2$ moiety of tyrosine.

The combination of this C2 isotope-sensitive radical EPR signal and the associated mass spectrometry showing a nonexchangeable H-atom abstraction from HPPA provides direct experimental confirmation of the proposal¹⁴ that the amino-nitrogen is the site of the H-atom abstraction for the native tyrosine substrate. Moreover, it is clear from these results that HPPA binds at the HydG substrate site with high fidelity. This encouraged us to consider the more oxidized coumaric acid, with a $\text{C}_2=\text{C}_3$ alkene substitution relative to HPPA, as another non-native substrate to test with rapid freeze quench EPR. Chemical intuition indicates that this substitution would raise the energy of any coumaric acid substrate radical formed in HydG relative to the now-characterized HPPA C2 centered radical. To put this on a more quantitative basis, the energetics for H-atom transfer for these substrates were examined with density functional theory (DFT) calculations at the $\omega\text{B97X-D}/6\text{-311+G(d,p)}$ level of theory (see SI section V for details).²⁷ As shown in Figure 3 (top trace), H-atom transfer from the amino group of tyrosine (zwitterion) is exergonic with a change in free energy between the two species (ΔG) of ~ -8 kcal/mol. The predicted barrier is ~ 13 kcal/mol. This primary tyrosine radical has so far eluded detection, although the 4-hydroxybenzyl radical product of its $\text{C}_\alpha-\text{C}_\beta$ bond lysis has been characterized in some detail.⁹ The DFT predictions for the $5'\text{dAdo}^\bullet$ radical's reaction with the non-native HPPA to produce a stable alkyl radical reveal a similar degree of exergonicity (center reaction) along with a slightly lower barrier (10.7 kcal/mol) compared to tyrosine and also reveal an ~ 0.99 spin density at the C2 carbon consistent with our EPR analysis. However, the computational results for the alkenyl radical generated from the $5'\text{dAdo}^\bullet$ radical's reaction with *cis-p*-coumaric acid (bottom reaction) are quite different. Although the barrier height for the H-atom transfer reaction is similar (~ 13 kcal/mol), the net free energy difference is negligible ($\Delta G = +0.1$ kcal/mol). This calculation does not take into account specifics of the protein binding sites for the different non-native substrates, currently unknown, but the fact that a near unity equilibrium constant is predicted for this "vacuum" reaction provides a thermodynamic justification for exploring the HydG reaction with the two isomers of coumaric acid as a potential enzymatic route to trap the $5'\text{dAdo}^\bullet$ radical.

In this regard, our approach is directly analogous to that of prior experiments probing radical SAM reactions employing chemically modified SAM, specifically *S*-3',4'-anhydroadenosyl-L-methionine (3',4'-anAdoMet) (anSAM),^{28,29} which provides allylic stabilization of its $5'$ -carbon centered radical relative to SAM itself. When employed with the rSAM enzyme lysine 2,3-aminomutase (LAM), the enzyme activity was greatly reduced but not zero ($\sim 0.25\%$), and the 3',4'-anhydro- $5'$ -deoxyadenosyl radical was in turn trapped and characterized via EPR, with the assignment to this modified SAM radical confirmed with appropriate isotopic substitu-

tions.^{28,29} In the case of these anSAM studies, a radical of a SAM analogue with a lower potential than the unmodified SAM radical was trapped when paired with the LAM enzyme's native substrate. The altered energetics of the pair results in slow H-atom abstraction and the trapping of a significant population of the 3',4'-anhydro- $5'$ -deoxyadenosyl radical. Our approach here is analogous, but complementary. We are using SAM itself, but pairing it with a higher potential non-native substrate, coumaric acid, with the goal of trapping the actual $5'\text{dAdo}^\bullet$ radical.

Experiments with *trans-p*-coumaric acid as a non-native substrate afforded no new radical EPR signals: only the HydG FeS signals were observed. Using LC-MS, we identified the generation of dAdoH when *cis-p*-coumaric acid is used as a substrate (Figure S6). From this, we know that this adenosyl radical decays and dAdoH is formed. Concurrent with the decay of this adenosyl radical, an axial $g_1 = 2.078$ EPR signal appears. This signal is both SAM and *cis-p*-coumaric acid dependent, and thus we believe this to be a downstream product of H-atom abstraction from *cis-p*-coumaric acid which leads to the generation of dAdoH.

However, the HydG reaction with *cis-p*-coumaric acid also generates a new CW EPR radical spectrum with a different pattern of ^1H hyperfine couplings than observed with HPPA (Figure 2C) (<10 s freeze quench time). At low EPR observation temperature (e.g., 10 K), we observe a set of overlying EPR spectra, including contributions from the two Fe-S clusters for HydG (Figure S7). (Assignments of all the EPR signals associated with the HydG *cis-p*-coumaric acid reaction will be the focus of an upcoming manuscript.) At relatively high observation temperatures ($\sim 40\text{--}60$ K), this new radical signal is clearly seen. Contributions from other species can be suppressed by subtracting the spectrum taken at 60 K from the spectrum at 40 K, with amplitudes weighted by the relative ($1/T$) Curie factors (Figure S8). To discriminate between a possible *cis-p*-coumaric acid centered radical or a SAM-derived radical, we repeated the freeze quench EPR with SAM fully ^{13}C -labeled in the adenosine moiety. The CW EPR spectrum is appreciably broadened (by about 8.5 mT) by multiple ^{13}C interactions, with some partially resolved hyperfine features (Figure 2D). These results clearly demonstrate that the rSAM reaction of HydG with *cis-p*-coumaric acid generates some form of adenosyl radical.

We note that the addition of the $5'\text{dAdo}^\bullet$ radical to terminal alkenes has been observed using Tyr analogues other than C2-*cis-p*-coumaric acid.³⁰ No additional broadening is observed in the EPR spectra of dAdo when ^{13}C -*cis-p*-coumaric acid is used in the HydG reaction (Figure S9), indicating that this new adenosyl radical does not correspond to such an addition product.

In order to better determine the distribution of spin density of the detected adenosyl radical and to specifically address whether we have trapped the $5'\text{dAdo}^\bullet$ radical, we carried out another *cis-p*-coumaric acid HydG reaction with SAM specifically deuterated at the four hydrogens bound to the C5', C4', and C3' carbons (Figure 4). This results (trace B) in a full collapse of proton hyperfine structure, showing that the spin density of the trapped adenosyl radical is localized in the vicinity of C5' as expected for the $5'\text{dAdo}^\bullet$ radical. The hyperfine structure of the SAM-derived radical signal is well simulated (Figure 4A, red trace) with three proton hyperfine interactions. The associated hydrogens must be bound to the C5', C4', and/or C3' of the ribose moiety of SAM, as when

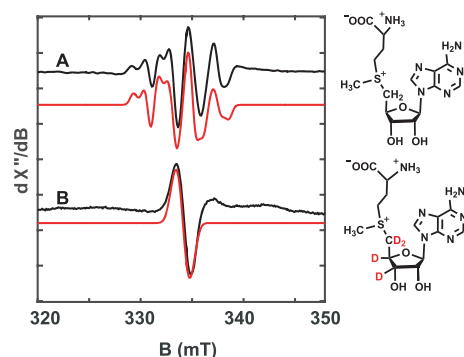


Figure 4. X-band CW of the $5'd\text{Ado}^\bullet$ generated in HydG. The subtraction spectra of the reaction mixture of HydG 100 μM , DTH 1 mM, *cis-p*-coumaric acid 300 μM , and (A) N.A. SAM, (B) *S*-adenosyl- $5',S',4',3'$ - 2H -methionine, 300 μM . Spectrometer configuration: frequency 9.4 GHz, power 2 mW. Spectra (A) and (B) are generated by subtracting the scaled spectra acquired at 60 K (accounting for a $1/T$ signal intensity dependence) from the spectra acquired at 40 K to remove a fast relaxing unassigned signal. Red traces in (A) and (B) are simulations using the same g -tensor [2.006 2.004 2.002]. (A) is simulated with three protons hyperfine tensors and corresponding Euler angles $A(\text{H}5'_{\text{endo}}) = [-25 \ -58 \ -107]$, Euler angle $(\text{H}5'_{\text{endo}}) = [0 \ -92 \ -46]^\circ$; $A(\text{H}5'_{\text{exo}}) = [-25 \ -58 \ -107]$, Euler angle $(\text{H}5'_{\text{exo}}) = [45 \ 126 \ 74]^\circ$, $A(\text{H}4') = [69 \ 62 \ 79]$, Euler angle $(\text{H}4') = [60 \ -60 \ -75]^\circ$. D4-SAM parameters are the same but with $\text{H}5'_{\text{endo}}$, $\text{H}5'_{\text{exo}}$ and $\text{H}4'$ scaled to deuterium hyperfine tensors by the ratio of their larmor frequencies $\gamma(^2\text{H})/\gamma(^1\text{H}) = 0.153$. $A(\text{D}5'_{\text{endo}}) = [-3.8 \ -8.9 \ -16.5]$ $A(\text{D}5'_{\text{exo}}) = [-3.8 \ -8.9 \ -16.5]$, $A(\text{D}4') = [10.6 \ 9.5 \ 12.15]$.

these are replaced by deuterons, the resolved proton hyperfine couplings are eliminated.

The ribose ^1H hyperfine simulation parameters (caption of Figure 4) can be used to calculate spin densities at the corresponding carbon. If we tentatively assign the two largest ^1H hyperfine couplings used in the simulation, both with hyperfine matrices of $|[-25 \ -58 \ -107]|$ (MHz), with an $|a_{\text{iso}}|$ of 63 MHz, we can use the McConnell relationship²⁶ between the carbon $2p_z$ spin density and the observed ^1H a_{iso} value (vide supra): This corresponds to $\sim 100\%$ spin density on the $\text{C}5'$ carbon ($\rho(\text{C}5') = 1.0$).

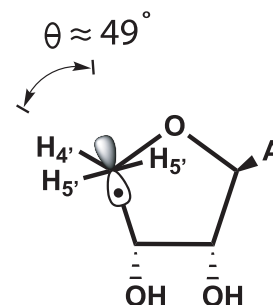
We then model the third ^1H hyperfine coupling in the simulation to the single $\text{C}4'$ hydrogen. With $\sim 100\%$ of the spin density in our model assigned to $\text{C}5'$, the coupling on this $\text{C}4'$ hydrogen $a_{\text{iso}}(\text{H}4') = 70$ MHz, arises via an orientation-dependent hyperconjugation mechanism, which can be calculated with another McConnell relation,³¹ specified for our model as

$$a_{\text{iso}}(\text{H}4') = \rho_{\text{C}5'} B'' \cos^2(\theta)$$

where $B'' = 162$ MHz and θ is the dihedral angle between the $\text{C}4'$ -H bond and the vector normal to angular node on the semi occupied p orbital of $\text{C}5'$ (Scheme 2). Given our assignment of $\rho(\text{C}5') \approx 1.0$, this expression provides a dihedral angle of $\theta \approx 49^\circ$ to rationalize the third measured ^1H coupling. The fourth isotopically exchanged hydrogen nucleus probed in our isotope substitution EPR experiment, on the $\text{C}3'$ carbon, has a hyperfine coupling to the spin density on $\text{C}5'$ too small to affect the CW EPR spectrum and is thus not required in the simulation.

We have not been able to obtain the single labeled $^{13}\text{C}5'$ -SAM, but we can get some estimate of the largest ^{13}C hyperfine component (~ 240 MHz) from the line broadening

Scheme 2. A Depiction down the $\text{C}5'$ - $\text{C}4'$ Bond of the Ribose Moiety of $5'd\text{Ado}^\bullet$, Showing the Dihedral Angle (θ) between the Singly Occupied p_z Orbital of $\text{C}5'$ and the $\text{C}4'$ -H Bond



of the CW EPR spectrum obtained with *S*-adenosyl-(2,4,5,6,8,1',2',3',4',5'- $^{13}\text{C}_{10}$)-methionine as described in the SI, section IV. We cannot extract the full ^{13}C hyperfine tensor from the CW EPR spectrum, but an estimate based on the ^{13}C line broadening, assuming it is dominated by the $^{13}\text{C}5'$ interaction, gives $\rho(\text{C}5') \approx 0.90(0.1)$, consistent with the large $\text{C}5'$ spin density obtained from the ^1H hyperfine analysis. In total, the EPR results with isotopically labeled SAM used with HydG in conjunction with *cis-p*-coumaric acid as a non-native substrate (Figures 2C,D and 4) provide a consistent assignment to the trapped $5'd\text{Ado}^\bullet$ radical, with its hallmark near-unity spin density on the $\text{C}5'$ carbon ($\rho(\text{C}5') \approx 1.0$).

This appears to be the first isotopically verified trapping and characterization of the $5'd\text{Ado}^\bullet$ radical in an actual rSAM enzymatic reaction, accomplished here by using a non-native substrate, *cis-p*-coumaric acid, in place of the native substrate tyrosine. As noted by Magnusson et al.,²⁹ the fact that the $5'd\text{Ado}^\bullet$ has never been directly observed spectroscopically in a radical SAM reaction makes its existence “hypothetical”, although their studies trapping the modified anSAM radical certainly provided prior support. We estimate based on analysis (SI section III) of the CW EPR spectra of Figure 2 that the $5'd\text{Ado}^\bullet$ radical generated with *cis-p*-coumaric acid builds to about one-fourth the concentration of the strong HPPA radical, roughly consistent with our thermodynamic prediction. The concentrations are calculated to be 4 μM and 16 μM for the $5'd\text{Ado}^\bullet$ radical and the HPPA radical, respectively (SI section IV), although we note using spin quantitation to compare species with different relaxation properties can induce a relatively high degree of error. Also, our trapping of the $5'd\text{Ado}^\bullet$ radical in HydG by using *cis-p*-coumaric acid as a non-native substrate with a relatively high radical state energy explicitly shows that the $5'd\text{Ado}^\bullet$ radical exists as a “free” radical in this reaction, although it may be possible that the organometallic “Omega” species exists early in the reaction.^{32,33} The only organic products detected in the reaction of *cis-p*-coumaric acid is $d\text{AdoH}$, thus the ultimate fate of the product of H-atom abstraction from *cis-p*-coumaric acid is currently unknown.

We note that a prior assignment of $5'd\text{Ado}^\bullet$ trapped in the C140A mutant of the radical SAM enzyme (RSE) spore photoproduct lyase (SPL)³⁴ lacked the specific magnetic isotope data needed to definitively assign the EPR spectrum. In fact, this spectrum is distinctly different from our isotope-verified $5'd\text{Ado}^\bullet$ radical shown here, or that of the $5'd\text{Ado}^\bullet$ radical generated by cryophotolysis,⁴ but its approximate 1:4:6:4:1 intensity ratio of the EPR spectrum and the

corresponding ^1H HFI gives an EPR signal that matches closely those found in gamma-irradiated crystals of derivatized L-alanine,^{35–37} suggesting that the reaction in this Cys-to-Ala mutant of SPL could lead instead to the formation of an alanine radical at position 140. Similarly, Downs and co-workers trapped a peptide backbone radical when initiating the radical SAM reaction in ThiC in the absence of substrate.³⁸

These examples illustrate that rSAM enzymes must exercise exquisite control or else the $5'\text{dAdo}^\bullet$ radical will rapidly quench itself at the expense of the protein, although an exception to this principle has been observed with NosL.³⁹ In the case of our HydG reaction with non-native substrates HPPA and *cis-p*-coumaric acid, our EPR results show that they bind sufficiently tightly in the native tyrosine substrate site that they are the targets of the $5'\text{dAdo}^\bullet$ H-atom abstraction, rather than having some protein site participating in a side reaction. Specifically, the C2-centered radical formation of HPPA suggests that this non-native substrate is binding in a similar geometry as tyrosine, as the C2 position in HPPA closely corresponds to the amino group position of tyrosine. Then, the fact that switching to a related non-native substrate, *cis-p*-coumaric acid with a double bond introduced adjacent to this C2 position, stabilizes the $5'\text{dAdo}^\bullet$ radical as not seen before in any rSAM enzyme reaction, points to specific binding for this non-native substrate, particularly in contrast to the trans isomer which does not generate this radical. We have introduced a thermodynamic argument for our success in trapping the $5'\text{dAdo}^\bullet$ radical, modeled closely on the prior anSAM studies.^{28,29} There may be more subtle substrate-binding issues at play, resulting in changes in the detailed kinetics between tyrosine and the two non-native substrates employed in this study, but until we have structures for HydG with these non-native substrates bound along with the native tyrosine (currently only modeled based on the NosL tryptophan binding motif^{14,15}), it will be difficult to rigorously assay these effects.

Another approach to generate the $5'\text{dAdo}^\bullet$ radical is direct photolysis of preformed SAM-metal complexes. It is well-known that the cobalt–carbon bond of cobalamins can be cleaved by light.^{40–42} Van Willigen and co-workers⁴³ used Fourier transform (pulse)-EPR and chemically induced dynamic electron polarization (CIDEP) to examine the radical pair products of photolysis and homolytic cleavage of the Co–C bond in methylcobalamin and $5'$ -adenosylcobalamin, and assigned resultant spectra to methyl and $5'\text{dAdo}^\bullet$ radicals, respectively (but see discussion questioning this assignment⁴). Now we have the isotopically verified $5'\text{dAdo}^\bullet$ generated by low-temperature photolysis of the prerduced [4Fe-4S]-SAM cluster of the rSAM enzyme pyruvate formate-lyase, along with its attendant EPR/ENDOR/DFT characterization.⁴ The CW EPR line shape of our $5'\text{dAdo}^\bullet$ radical produced by the HydG reaction with *cis-p*-coumaric acid is remarkably similar to this cryogenerated radical signal. Any small differences are likely attributable to differences in the C4'-H hyperfine coupling due to different dihedral angles (θ in our notation), no doubt resulting from the two different radical generation protocols. Moreover, the spectral changes induced by using various isotopically labeled SAMs in both set of experiments point to the same assignment of a $5'\text{dAdo}^\bullet$ radical, with the vast majority spin density at the C5' carbon, even though the specifics of the exact isotope labels are different between the two groups. As clearly described by Yang et al.,⁴ trapping and characterization of the “elusive” $5'\text{dAdo}^\bullet$ have been a long time

coming, and it is interesting that it can now be done by two different approaches, the cryoillumination method and the rSAM reaction with a non-native substrate, with essentially identical $5'\text{dAdo}^\bullet$ radicals resulting. Our approach, trapping the $5'\text{dAdo}^\bullet$ radical by altering the thermodynamics of its primary H-atom abstraction target using non-native substrates, should be a broadly applicable approach toward generating the $5'\text{dAdo}^\bullet$ radical in other rSAM enzymes, providing a nuanced probe of its conformation and electronic structure in different enzyme environments.

Safety. No unexpected or unusually high safety hazards were encountered in this research.

■ ASSOCIATED CONTENT

Supporting Information

The Supporting Information is available free of charge on the ACS Publications website at DOI: 10.1021/acscentsci.9b00706.

Trapping and EPR characterization of the $5'\text{dAdo}^\bullet$ radical in a radical SAM enzyme reaction with a non-native substrate (PDF)

■ AUTHOR INFORMATION

Corresponding Author

*E-mail: rdbritt@ucdavis.edu. Phone: (530) 752 6377.

ORCID

Troy A. Stich: 0000-0003-0710-1456

Sumedh Joshi: 0000-0002-0407-2920

Jared T. Shaw: 0000-0001-5190-493X

Tadhg P. Begley: 0000-0001-5134-2623

Dean J. Tantillo: 0000-0002-2992-8844

R. David Britt: 0000-0003-0889-8436

Present Address

‡(T.A.S.) Department of Chemistry, Wake Forest University, Winston-Salem NC, USA 27101.

Notes

The authors declare no competing financial interest.

■ ACKNOWLEDGMENTS

This work was supported by an NIH grant to the R.D.B. laboratory (1R35GM126961) and by grants from the Robert A. Welch Foundation (A-0034 to T.P.B.) and the National Science Foundation (1507191 to T.P.B.). D.J.T. gratefully acknowledges computational support from the NSF XSEDE program. T.A.S. acknowledges financial support from Wake Forest University.

■ REFERENCES

- (1) Frey, P. A.; Magnusson, O. T. S-Adenosylmethionine: A wolf in sheep's clothing, or a rich man's adenosylcobalamin? *Chem. Rev.* **2003**, *103*, 2129–2148.
- (2) Broderick, J. B.; Duffus, B. R.; Duschene, K. S.; Shepard, E. M. Radical S-Adenosylmethionine enzymes. *Chem. Rev.* **2014**, *114*, 4229–4317.
- (3) Bridwell-Rabb, J.; Grell, T. A.; Drennan, C. L. A rich man, poor man story of s-adenosylmethionine and cobalamin revisited. *Annu. Rev. Biochem.* **2018**, *87*, 555–584.
- (4) Yang, H.; McDaniel, E.; Impano, S.; Byer, A. S.; Jodts, R. J.; Yokoyama, K.; Broderick, W. E.; Broderick, J. B.; Hoffman, B. M. The elusive $5'$ -Deoxyadenosyl radical: captured and characterized by EPR and ENDOR spectroscopies. *J. Am. Chem. Soc.* **2019**, *141*, 12139–12146.

- (5) Pilet, E.; Nicolet, Y.; Mathevon, C.; Douki, T.; Fontecilla-Camps, J. C.; Fontecave, M. The role of the maturase HydG in FeFe-hydrogenase active site synthesis and assembly. *FEBS Lett.* **2009**, *583*, 506–511.
- (6) Driesener, R. C.; Challand, M. R.; McGlynn, S. E.; Shepard, E. M.; Boyd, E. S.; Broderick, J. B.; Peters, J. W.; Roach, P. L. FeFe-hydrogenase cyanide ligands derived from S-adenosylmethionine-dependent cleavage of tyrosine. *Angew. Chem., Int. Ed.* **2010**, *49*, 1687–1690.
- (7) Shepard, E. M.; Duffus, B. R.; George, S. J.; McGlynn, S. E.; Challand, M. R.; Swanson, K. D.; Roach, P. L.; Cramer, S. P.; Peters, J. W.; Broderick, J. B. FeFe-hydrogenase maturation: HydG-catalyzed synthesis of carbon monoxide. *J. Am. Chem. Soc.* **2010**, *132*, 9247–9249.
- (8) Shepard, E. M.; Mus, F.; Betz, J. N.; Byer, A. S.; Duffus, B. R.; Peters, J. W.; Broderick, J. B. FeFe-hydrogenase maturation. *Biochemistry* **2014**, *53*, 4090–4104.
- (9) Kuchenreuther, J. M.; Myers, W. K.; Stich, T. A.; George, S. J.; NejatyJahromy, Y.; Swartz, J. R.; Britt, R. D. A radical intermediate in tyrosine scission to the CO and CN- ligands of FeFe hydrogenase. *Science* **2013**, *342*, 472–475.
- (10) Kriek, M.; Martins, F.; Leonardi, R.; Fairhurst, S. A.; Lowe, D. J.; Roach, P. L. Thiazole synthase from *Escherichia coli* - An investigation of the substrates and purified proteins required for activity in vitro. *J. Biol. Chem.* **2007**, *282*, 17413–17423.
- (11) Kriek, M.; Martins, F.; Challand, M. R.; Croft, A.; Roach, P. L. Thiamine biosynthesis in *Escherichia coli*: Identification of the intermediate and by-product derived from tyrosine. *Angew. Chem., Int. Ed.* **2007**, *46*, 9223–9226.
- (12) Nicolet, Y.; Martin, L.; Tron, C.; Fontecilla-Camps, J. C. A glycyI free radical as the precursor in the synthesis of carbon monoxide and cyanide by the FeFe-hydrogenase maturase HydG. *FEBS Lett.* **2010**, *584*, 4197–4202.
- (13) Duffus, B. R.; Ghose, S.; Peters, J. W.; Broderick, J. B. Reversible H atom abstraction catalyzed by the radical S-adenosylmethionine enzyme HydG. *J. Am. Chem. Soc.* **2014**, *136*, 13086–13089.
- (14) Nicolet, Y.; Zeppieri, L.; Amara, P.; Fontecilla-Camps, J. C. Crystal structure of tryptophan lyase (NosL): Evidence for radical formation at the amino group of tryptophan. *Angew. Chem., Int. Ed.* **2014**, *53*, 11840–11844.
- (15) Dinis, P.; Suess, D. L. M.; Fox, S. J.; Harmer, J. E.; Driesener, R. C.; De La Paz, L.; Swartz, J. R.; Essex, J. W.; Britt, R. D.; Roach, P. L. X-ray crystallographic and EPR spectroscopic analysis of HydG, a maturase in FeFe-hydrogenase H-cluster assembly. *Proc. Natl. Acad. Sci. U. S. A.* **2015**, *112*, 1362–1367.
- (16) Diner, B. A.; Britt, R. D. In *Photosystem II: The Light-Driven Water-Plastoquinone Oxidoreductase*; Wydrzynski, T. J., Satoh, K., Freeman, J. A., Eds.; Springer Netherlands: Dordrecht, 2005; pp 207–233.
- (17) Bender, C. J.; Sahlin, M.; Babcock, G. T.; Barry, B. A.; Chandrashekar, T. K.; Salowe, S. P.; Stubbe, J.; Lindstrom, B.; Petersson, L.; Ehrenberg, A.; Sjöberg, B. M. An endor study of the tyrosyl free-radical in ribonucleotide reductase from *Escherichia coli*. *J. Am. Chem. Soc.* **1989**, *111*, 8076–8083.
- (18) Hulsebosch, R. J.; vandenBrink, J. S.; Nieuwenhuis, S. A. M.; Gast, P.; Raap, J.; Lugtenburg, J.; Hoff, A. J. Electronic structure of the neutral tyrosine radical in frozen solution. Selective H-2-, C-13-, and O-17-isotope labeling and EPR spectroscopy at 9 and 35 GHz. *J. Am. Chem. Soc.* **1997**, *119*, 8685–8694.
- (19) Minnihan, E. C.; Nocera, D. G.; Stubbe, J. Reversible, long-range radical transfer in E-coli Class la ribonucleotide reductase. *Acc. Chem. Res.* **2013**, *46*, 2524–2535.
- (20) Hofbauer, W.; Zouni, A.; Bittl, R.; Kern, J.; Orth, P.; Lendzian, F.; Fromme, P.; Witt, H. T.; Lubitz, W. Photosystem II single crystals studied by EPR spectroscopy at 94 GHz: The tyrosine radical Y-D[•]. *Proc. Natl. Acad. Sci. U. S. A.* **2001**, *98*, 6623–6628.
- (21) van der Donk, W. A.; Stubbe, J. Protein radicals in enzyme catalysis. *Chem. Rev.* **1998**, *98*, 2661–2662.
- (22) McEvoy, J. P.; Brudvig, G. W. Water-splitting chemistry of photosystem II. *Chem. Rev.* **2006**, *106*, 4455–4483.
- (23) Bhandari, D. M.; Xu, H.; Nicolet, Y.; Fontecilla-Camps, J. C.; Begley, T. P. Tryptophan lyase (NosL): Mechanistic insights from substrate analogues and mutagenesis. *Biochemistry* **2015**, *54*, 4767–4769.
- (24) Cole, T.; Pritchard, H. O.; Davidson, N. R.; McConnell, H. M. Structure of the methyl-radical. *Mol. Phys.* **1958**, *1*, 406–409.
- (25) Morton, J. R.; Preston, K. F. Atomic parameters for paramagnetic-resonance data. *J. Magn. Reson.* **1978**, *30*, 577–582.
- (26) McConnell, H. M.; Heller, C.; Cole, T.; Fessenden, R. W. Radiation damage in organic crystals 0.1. CH(COOH)₂ in malonic acid. *J. Am. Chem. Soc.* **1960**, *82*, 766–775.
- (27) Sengupta, A.; Raghavachari, K. Solving the density functional conundrum: Elimination of systematic errors to derive accurate reaction enthalpies of complex organic reactions. *Org. Lett.* **2017**, *19*, 2576–2579.
- (28) Magnusson, O. T.; Reed, G. H.; Frey, P. A. Spectroscopic evidence for the participation of an allylic analogue of the 5'-deoxyadenosyl radical in the reaction of lysine 2,3-aminomutase. *J. Am. Chem. Soc.* **1999**, *121*, 9764–9765.
- (29) Magnusson, O. T.; Reed, G. H.; Frey, P. A. Characterization of an allylic analogue of the 5'-deoxyadenosyl radical: An intermediate in the reaction of lysine 2,3-aminomutase. *Biochemistry* **2001**, *40*, 7773–7782.
- (30) Wu, Y. J.; Wu, R. Z.; Mandalapu, D.; Ji, X. J.; Chen, T.; Ding, W.; Zhang, Q. Radical SAM-dependent adenylation catalyzed by L-tyrosine lyases. *Org. Biomol. Chem.* **2019**, *17*, 1809–1812.
- (31) Fessenden, R. W.; Schuler, R. H. Electron spin resonance studies of transient alkyl radicals. *J. Chem. Phys.* **1963**, *39*, 2147–2195.
- (32) Horitani, M.; Shisler, K.; Broderick, W. E.; Hutcheson, R. U.; Duschene, K. S.; Marts, A. R.; Hoffman, B. M.; Broderick, J. B. Radical SAM catalysis via an organometallic intermediate with an Fe-5'-C-deoxyadenosyl bond. *Science* **2016**, *352*, 822–825.
- (33) Byer, A. S.; et al. Paradigm shift for radical S-Adenosyl-L-methionine reactions: The organometallic intermediate Omega is central to catalysis. *J. Am. Chem. Soc.* **2018**, *140*, 8634–8638.
- (34) Heidinger, L.; Kneutinger, A. C.; Kashiwazaki, G.; Weber, S.; Carell, T.; Schleicher, E. Direct observation of a deoxyadenosyl radical in an active enzyme environment. *FEBS Lett.* **2016**, *590*, 4489–4494.
- (35) Sagstuen, E.; Hole, E. O.; Haugedal, S. R.; Nelson, W. H. Alanine radicals: Structure determination by EPR and ENDOR of single crystals X-irradiated at 295 K. *J. Phys. Chem. A* **1997**, *101*, 9763–9772.
- (36) Heydari, M. Z.; Malinen, E.; Hole, E. O.; Sagstuen, E. Alanine radicals. 2. The composite polycrystalline alanine EPR spectrum studied by ENDOR, thermal annealing, and spectrum simulations. *J. Phys. Chem. A* **2002**, *106*, 8971–8977.
- (37) Baskan, M. H.; Aydin, M.; Osmanoglu, S.; Topkaya, R. Electron paramagnetic resonance characterization of gamma irradiation damage centers in powder of L-(+)-tartaric acid, N-acetyl-L-alanine and L-methyl-L-histidine. *Radiat. Eff. Defects Solids* **2010**, *165*, 938–943.
- (38) Martinez-Gomez, N. C.; Poyner, R. R.; Mansoorabadi, S. O.; Reed, G. H.; Downs, D. M. Reaction of adomet with ThiC Generates a backbone free radical. *Biochemistry* **2009**, *48*, 217–219.
- (39) Bhandari, D. M.; Fedoseyenko, D.; Begley, T. P. Tryptophan lyase (NosL): A cornucopia of 5'-deoxyadenosyl radical mediated transformations. *J. Am. Chem. Soc.* **2016**, *138*, 16184–16187.
- (40) Schrauzer, G. N.; Lee, L. P.; Sibert, J. W. Alkylcobalamins and alkylcobaloximes - electronic structure, spectra, and mechanism of photodealkylation. *J. Am. Chem. Soc.* **1970**, *92*, 2997–3005.
- (41) Golding, B. T.; Kemp, T. J.; Sellers, P. J.; Nocchi, E. Anaerobic photodecomposition of alkylaquocobaloximes in aqueous-solution. *J. Chem. Soc., Dalton Trans.* **1977**, 1266–1272.
- (42) Mok, C. Y.; Endicott, J. F. Photochemistry of organocobalt complexes containing tetraaza macrocyclic ligands - cobalt-methyl homolysis and nature of cobalt-carbon bond. *J. Am. Chem. Soc.* **1978**, *100*, 123–129.

(43) Bussandri, A. P.; Kiarie, C. W.; Van Willigen, H. Photoinduced bond homolysis of B-12 coenzymes. An FT-EPR study. *Res. Chem. Intermed.* **2002**, *28*, 697–710.

(44) Suess, D. L. M.; Buerstel, I.; De La Paz, L.; Kuchenreuther, J. M.; Pham, C. C.; Cramer, S. P.; Swartz, J. R.; Britt, R. D. Cysteine as a ligand platform in the biosynthesis of the FeFe hydrogenase H cluster. *Proc. Natl. Acad. Sci. U. S. A.* **2015**, *112*, 11455–11460.